

Effect of V and Ni addition on the Ti-Pt shape memory alloys for high temperature applications

Rosinah. Modiba^{1,2*}

^{1*}Advanced Materials Engineering, Manufacturing, Council for Scientific and Industrial Research, PO Box 395, Pretoria, 0001, South Africa,

²Department of Physics, Sefako Makgatho Health Sciences University, P.O Box 94, Ga-Rankuwa 0204, South Africa

Abstract. Currently, high temperature shape memory alloys (HTSMA) are in great demand for their development and commercialization. The titanium-platinum (TiPt) alloy is the most attractive and promising HTSMA for aerospace and automobile applications due to its high transformation temperature of above 1300 K. The binary TiPt alloy has been found to show a limited shape memory capacity due to a lower critical stress needed for slip deformation rather than martensitic transformation. Incorporating alloying elements has been recommended as a method to enhance both the mechanical properties and shape memory effect of the binary TiPt alloy but may alter the transformation temperature. In this study, the effect of vanadium (V) and nickel (Ni) on the B2 TiPt alloy is investigated using first principle approach. The structural and elastic properties of the alloys are determined. The addition of both V and Ni was found to be stabilizing the cubic beta phase with a positive tetragonal shear C' observed. In addition, the density of states of the structures are presented.

1 Introduction

Titanium-based shape memory alloys (SMAs) are commonly utilized in engineering and medicine because of their good shape memory effect and super-elasticity during martensitic transformations [1]. Alloys that have shape memory can recall their initial form with the application of specific pressure or temperature. It is claimed that SMAs demonstrate a martensitic transformation that is reversible in terms of crystal structure. During high temperatures, the Shape Memory Alloy (SMA) is present in an austenite phase with long-range order that shifts to a martensite phase when it cools down. Some of the applications include actuators and medical stents [2, 3]. An increasing need exists for high temperature SMAs suitable for elevated temperature settings, with only a few options currently showing promise, such as Ti (Ni,Pt) [4, 5] and Ti (Ni,Pd) [6, 7]. Nevertheless, the martensitic transformation temperature (T_m) of the majority of shape memory alloys still stayed under 830 K even after adding ternary alloys [5]. The study aims to develop shape memory alloys with a martensitic transformation (T_m) temperature of 1000 K and above.

*Corresponding author: Rmahlangu1@csir.co.za.

The Ti-Pt alloys experience a B2-B19 martensite phase change at a transition temperature over 1300 K [8]. Nevertheless, it has been noted that Ti-Pt based alloys show a minimal shape memory effect because of a lower critical stress for slip deformation in comparison to the stress needed for martensitic transformation [9, 10]. Therefore, it is crucial to improve the mechanical characteristics of the equi-atomic TiPt alloy in order to make it suitable for use in elevated temperatures. The work on the partial substitution of the third element into the shape memory alloy systems has been done previously using both experimental and computational approaches [11, 12]. The elastic properties and electronic structure of B2 TiNi with the addition of three alloying elements, Fe, Cu and Pd have been investigated using the first-principles [13]. The addition of Cu suggested a B2 to B19' martensitic transformation whereas both Fe and Pd reduced the B19' transformation temperature of the B2 TiNi. In addition, the experimental work reported on the $Ti_{50}Pd_{50-x}Ni_x$ [14] suggested that the substitution of Pd with Ni increases its martensitic temperature. Wadood and Mitarai reported on the effect of partial substitution of Pt with Co and Ru on the Ti-50Pt [15]. Furthermore, the work on TiPt-V reported by R. Modiba et.al [16] showed that vanadium addition on the TiPt alloy stabilized the alloys with a reduced transformation temperature. The same was observed on the DSC work reported by S. Chikosha et.al. [17]. They found that as much as the temperature of the $Ti_{50}Pt_{43.75}V_{6.25}$ alloy was reduced, the ternary alloy remained as a B19 phase upon cooling.

In this study, the first principle approach is used to investigate the effect of vanadium and nickel on the B2 TiPt alloys. Prior research on the substitution of V showed that it enhanced the stability of TiPt alongside commercial TiNi alloys, leading to improved mechanical properties when combined with TiPt. The alloys' stability is assessed based on their lattice parameters, elastic constants, and density of states.

2 Methodology

In this work, the density functional theory (DFT) [18, 19] formalism as implemented in CASTEP [20] was employed to investigate the stability of the B2 TiPt structure alloyed with both V and Ni elements on the Pt side with the projector augmented wave (PAW) [21]. A cut-off energy of 500 eV was employed because it was enough to achieve convergence in the total energy of the configurations.

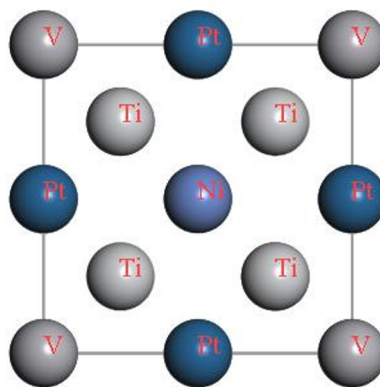


Fig. 1: The cubic B2 Ti (Pt-V-Ni) structure.

The Perdew-Burke-Ernzerhof (PBE) [22] generalized gradient approximation was used for the exchange-correlation functional. The k-point meshes of 8x8x8 were used for geometry optimization according to Monkhorst-Pack [23]. A 2x2x2 supercell of the cubic B2 TiPt with 16 atoms was used to alloy with V and Ni and the sample structure is shown in Figure 1 below. The standards for structure optimization and energy calculation were adjusted to high precision, with the tolerance for the stress concentration factor (SCF), energy, maximum force, and maximum displacement all set to 1.0×10^{-5} eV per atom, 0.03 eV per Angstrom, and 0.001 Angstrom, respectively. All the computations were performed at 0 Kelvin.

3 Results and discussions

3.1 Lattice parameters, elastic constants and mechanical properties

The lattice parameters of the cubic B2 $Ti_8VPt_3Ni_4$, $Ti_8VNi_3Pt_4$ and $Ti_8Pt_3Ni_3V_2$ structures were determined and are plotted in Figure 2(a). It can be noted from the graph, that $Ti_8VPt_3Ni_4$ has the largest lattice parameter compared to other structures which can be attributed to larger number of nickel atoms in the system compared to Pt. In Figure 2(b) the plots of the calculated heats of formation (ΔH_f) for the structures are shown. The following equation was used to calculate the ΔH_f :

$$\Delta H_f = E_c - \sum_i x_i E_i \quad (1)$$

where E_c is the calculated total energy of the compound, E_i is the calculated total energy of element i in the compound. The structure of $Ti_8VNi_3Pt_4$ is found to be thermodynamically stable with the lowest heats of formation. The least stable structure with the lowest ΔH_f is found to be $Ti_8Pt_3Ni_3V_2$ with a value of -0,60 eV as depicted in Figure 2(b) below.

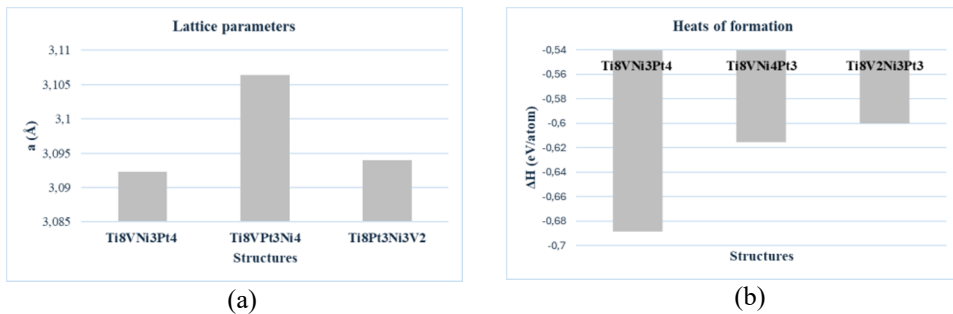


Fig. 2 : The graphs of (a) equilibrium lattice parameters and (b) heats of formation of the structures.

To further understand the mechanical stability of the alloys, their elastic constants and mechanical properties were investigated and presented in Table 1. Cubic structures have three independent elastic constants (C_{11} , C_{12} , C_{44}). The system for determining mechanical stability criteria [24] is given as follows:

$$C_{44} > 0, C_{11} > |C_{12}| \text{ and } C_{11} + 2C_{12} > 0 \quad (1)$$

$$C' = (C_{11} - C_{12})/2 \quad (2)$$

$$A = \frac{C_{44}}{C'} \quad (3)$$

All the C_{ij} 's of the structures were found to obey the stability criterion in Equation (1) suggesting that the structures are mechanically stable. The anisotropy (A) of the structures were also calculated using equation (3) and their values are found to be smaller than those of the known martensitic alloys such as CuZn and NiAl [25]. The results show that at the higher concentration of V, the anisotropy is approaching unity suggesting that there is a coupling between the C_{44} and C' at this concentration as illustrated by their values in Table 1.

Table 1. The determined elastic properties C_{ij} 's (GPa), bulk modulus B (GPa), shear modulus G (GPa), Young's modulus E (GPa), C' , anisotropy (A), Poisson's ratio ν , Vickers hardness (Hv), G/B of the structures.

Properties	Ti ₈ VNi ₄ Pt ₃	Ti ₈ VNi ₃ Pt ₄	Ti ₈ V ₂ Ni ₃ Pt ₃
c_{11}	204	199	170
c_{44}	58	50	54
c_{12}	167	153	77
c'	18	23	46
A	3.17	2.21	1.16
Bulk	180	169	108
Shear	37	37	51
G/B	0.20	0.22	0.47
E	103	102	131
ν	0.40	0.39	0.29
Hv	1.95	2.07	6.27

The increase of the anisotropy is observed at Ti₈VPt₃Ni₄ which is due to the decrease in C' . It is argued that higher A is a sufficient condition for B2-B19 martensitic transformation. However, smaller A indicates that there is a stronger correlation between C_{44} and C' . The addition of both V and Ni to the TiPt phase increases the C' and this results in the phase being mechanically stable as opposed to the previously calculated results ($C' = -32$) [26]. The calculated anisotropy of all the structures are presented in Table 1 and the A of the Ti₈V₂Pt₃Ni₃ is found to smaller with a value of 1.16 closer to unity, suggesting a B2-B19' transformation [26].

To investigate the ductility, hardness and plasticity of the structures, their changes in shear (G), bulk (B), Young's (E) moduli, and Poisson's ratio (ν) were compared. The shear modulus of Ti₈V₂Pt₃Ni₃ was higher than other structures with a value of 51 GPa, suggesting that the alloy is rigid. The bulk modulus, Poisson's ratio and the Vicker's hardness values of both Ti₈VPt₃Ni₄ and Ti₈VNi₃Pt₄ are comparable as seen in Table 1.

Pugh [27] proposed an empirical criterion that requires G/B to be less than 0.57 for ductile metals. All the compositions satisfy the ductility conditions since all G/B values are less than 0.57. Another requirement for ductility in metals is that the anisotropy factor must exceed 0.8, while Poisson's ratio should be below 0.35 [28]. The calculated Poisson's ratio of the Ti₈Pt₃Ni₃V₂ was found to be less than 0.35, suggesting the structure's ductility compared to others with values greater than 0.35. In addition, the anisotropy of the alloys is more than 0.8.

Multiple macroscopic empirical models link material hardness to elastic coefficients [29]. Hardness was assessed using the Tian formula, which defines hardness in relation to the polycrystalline bulk, B, and shear, G, moduli (using Pugh's modulus ratio, $k=G/B$):

$$H_V = 0.92k^{1.137}G^{0.708} \quad (4)$$

The macroscopic model shows a strong correlation with experimental hardness values above 5 GPa, but tends to overestimate the hardness of softer materials. The calculated hardness of the $Ti_8Pt_3Ni_3V_2$ is found to be 6.27 GPa greater than 5 GPa. The results suggest that $Ti_8Pt_3Ni_3V_2$ is hard and ductile compared to the $Ti_8VPt_3Ni_4$ and $Ti_8VNi_3Pt_4$ structures.

3.2 Density of states

To determine the electronic properties of the structures, the density of states profile has been generated. The total density of states (TDOS) and partial density of states (PDOS) curves for $Ti_8VPt_3Ni_4$, $Ti_8VNi_3Pt_4$, and $Ti_8Pt_3Ni_3V_2$ structures are presented in Figure 3 below.

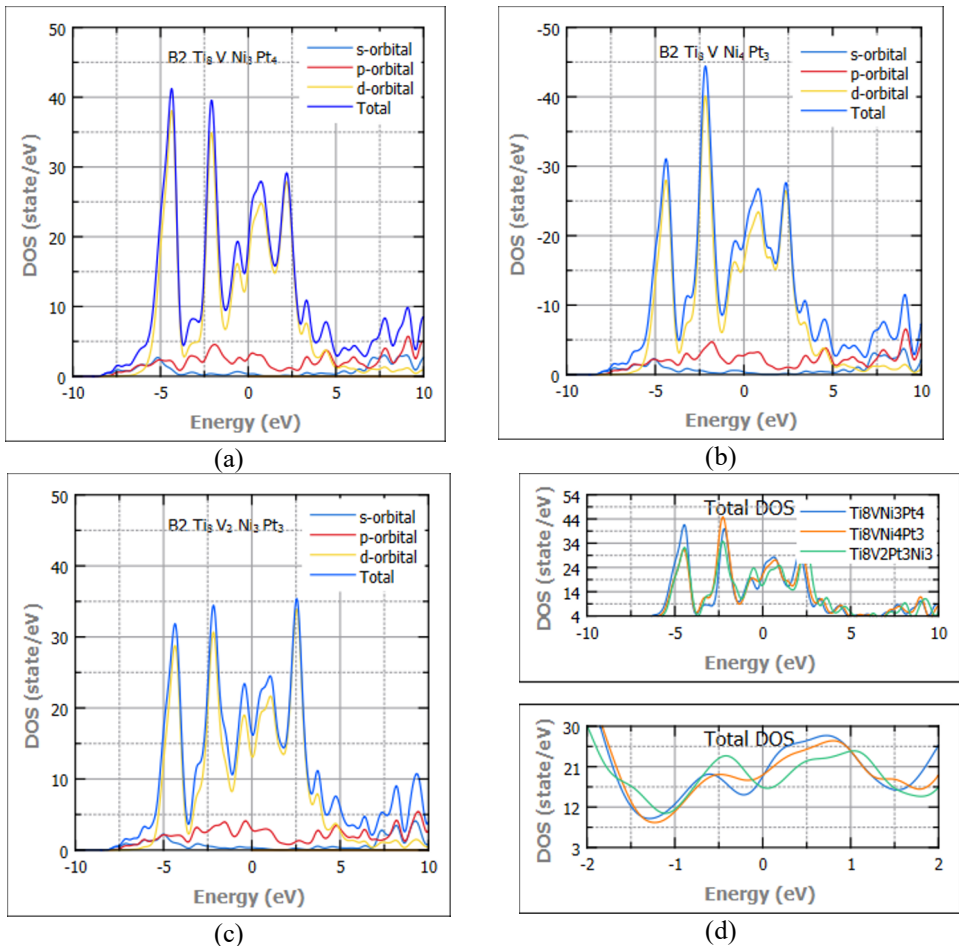


Fig. 3: The density of states of (a) $Ti_8VNi_3Pt_4$, (b) $Ti_8VPt_3Ni_4$ (c) $Ti_8Pt_3Ni_3V_2$, and (d) their total DOS plots embedded.

Both s and p orbitals contribute minimally to the TDOS of the structures as compared to the d orbitals. The lowest total DOS at Fermi level (E_f) corresponds to a more stable structure, while a high TDOS implies less stability. The E_f of both $Ti_8VNi_4Pt_3$ and $Ti_8VNi_3Pt_4$ hits the TDOS at the left side of the $Ti_8VNi_3Pt_4$ shoulder with $Ti_8VNi_3Pt_4$ having the highest value of TDOS.

Furthermore, the Fermi level in Figure 3 (c) is seen to be hitting the d-orbital in the deep contributing to the total DOS energy of the $Ti_8V_2Ni_3Pt_3$ curve. Figure 3 (d) presents the embedded total DOS plots of the structures for better comparison at Fermi level with the zoomed-in plots at Fermi energy which is taken as the energy at zero ($E-E_f=0$). It can be seen in the plots that $Ti_8Pt_3Ni_3V_2$ is the most stable structure with the lowest TDOS at the Fermi level with $Ti_8VPt_3Ni_4$ being the least stable with the highest number of TDOS at E_f .

4 Conclusions

The density functional theory was used to investigate the effect of both V and Ni on the cubic TiPt alloy. The stability of the three structures namely: $Ti_8VNi_4Pt_3$, $Ti_8VNi_3Pt_4$ and $Ti_8V_2Ni_3Pt_3$ were investigated. The structural, elastic properties and density of states were determined for the structures. It was observed that the $Ti_8VNi_4Pt_3$ structure is the most thermodynamically stable with the lowest heats of formation as compared to the other structures with $Ti_8V_2Ni_3Pt_3$ being the least. Furthermore, $Ti_8V_2Ni_3Pt_3$ satisfied all the ductility conditions of metals as determined using both the elastic constants and the mechanical properties calculations. Both $Ti_8VNi_4Pt_3$ and $Ti_8VNi_3Pt_4$ structures behaved similarly with comparable values of their mechanical properties. The study predicts $Ti_8V_2Ni_3Pt_3$ alloy to be a potential alloy for applications as a shape memory alloy. Further investigations into the transformation temperatures of the alloys will be studied using an experimental approach.

The Accelerated Principal Researcher Developmental Program (APRDP) from the Council for Scientific and Industrial Research (CSIR) and the Advanced Materials and Manufacturing Program from Department of Science and Innovation (DSI) are acknowledged for their financial support. The calculations were carried out using computer resources at the Centre for High-Performance Computing (CHPC) in CSIR Cape Town.

References

- [1] K. Otsuka and C.M. Wayman, "Shape Memory Materials," Cambridge, Cambridge University Press, 220 (1998).
- [2] M.H. Wu and L. M. Schetky, "Industrial Applications For Shape Memory Alloys," in *SMST*, California, (2000).
- [3] K. Otsuka and T. Kakeshita, "Science and Technology of Shape-Memory Alloys: New Developments," *MRS Bull*, **27**, 91 (2002).
- [4] Y. Takahashi, T. Inamura, J. Sakurai, H. Hosoda, K. Wakashima and S. Miyazaki, *Trans. MRS-J.*, **29**, 3005 (2004).
- [5] T. Inamura, Y. Takahashi, H. Hosoda, K. Wakashima, T. Nagase, T. Nakano, Y. Umakoshi and S. Miyazaki, *MRS*, **842**, 347 (2004).
- [6] Y. Suzuki, Y. Xu, S. Morito, K. Otsuka and K. Mitose, "Effects of Boron Addition on Microstructure and Mechanical Properties of Ti–Ti–Ni High-Temperature Shape Memory Alloys," *Mater. Lett.*, vol. **36**, 85 (1998).
- [7] S. Shimizu, Y. Xu, E. Okunishi, S. Tanaka, K. Otsuka and K. Mitose, *Mater. Lett.*, no. **34**, 23 (1998).
- [8] H.C. Donkersloot and J.H.N. Van Vucht, *J. Less-Common Met.*, **20**, 83 (1970).
- [9] Y. Yamabe-Mitarai, T. Hara, S. Miura, H. Hosoda, *Mater. Trans.*, vol. **47**, 650–657 (2000).
- [10] Y. Yamabe-Mitarai, T. Hara, S. Miura, H. Hosoda, *Intermetallics*, **18**, 2275 (2010).

- [11] C. Tan, X Tian, and W. Cai, “Martensitic Transformation of TiNiPd High-Temperature Shape Memory Alloys: A first-Principles Study,” *Physica. B*, **404**, 3662 (2009).
- [12] A. Wadood, M. Takahashi, S. Takahashi, H. Hosoda, Y. Yamabe-Mitarai, “High-Temperature Mechanical and Shape Memory Properties of TiPt–Zr and TiPt–Ru Alloys,” *Mater. Sci. Eng. A*, **564**, 34 (2013).
- [13] W. Cai, C. Tan, T. Shen and X. Tian, “First-Principles Study on Alloying Effect on Martensitic Transformation Behavior of TiNi Alloy,” *J. Alloy Compd.*, **438**, 30 (2007).
- [14] D. Golberg, Ya. Xu, Y. Murakami, K. Otsuka, T. Ueki and H. Horikawa, “High-Temperature Shape Memory Effect in Ti50Pd50-xNix (x= 10, 15, 20) Alloys,” *Mat. Lett.*, **22**, 241 (1995).
- [15] A. Wadood and Y. Yamabe-Mitarai, “TiPt-Co and TiPt-Ru High Temperature Shape Memory Alloys,” *Mat. Sci. Eng. A*, **601**, 106 (2014).
- [16] R. Modiba, E. Baloyi, S. Chikosha, H.R Chauke, P.E Ngoepe, *IOP Conf. Ser.: Mater. Sci. Eng.* **430**, 012021 (2018)
- [17] S. Chikosha , M.L Mahlatji , R. Modiba , H.K Chikwanda , *IOP Conf. Ser.: Mater. Sci. Eng.* **430**, 012022 (2018).
- [18] P. Hohenberg and W. Kohn, *Phys. Rev. B*, **136**, 864 (1964).
- [19] W. Kohn and L. J. Sham, *Phys. Rev. A*, **140**, 1133 (1965).
- [20] S.J. Clark, M.D. Segall, C.J. Pickard, P.J. Hasnip, M.J. Probert, K. Refson and M.C. Payne, “First-principles Methods Using CASTEP,” *Z. Kristallographie*, **220**, 567 (2005).
- [21] P E. Blöchl, J. Kaestner, C J. Foerst, “Electronic structure methods: Augmented Waves, Pseudopotentials and the Projector Augmented Wave Method,” in *Handbook of Materials Modeling*, 0407205 (2004).
- [22] Joachim Paier, Robin Hirschl, Martijn Marsman, Georg Kresse, “The Perdew–Burke–Ernzerhof exchange–correlation functional applied to the G2-1 test set using a plane-wave basis set,” *J. Chem. Phys.*, **122**, 234102 (2005).
- [23] H.J. Monkhorst and J.D. Pack, *Phys. Rev. B*, **13**, 5188 (1976).
- [24] Wu ZJ, Zhao EJ, Xiang HP, Hao XF, Liu XJ, Meng , “Ab-Initio Calculation of the Elastic Constants and Thermal Expansion Coefficients of Laves Phases,” *J. Phys. Rev. B*, **76**, 054115 (2007).
- [25] J.A. Wollmershauser, S. Kabra, S.R. Agnew, “In Situ Neutron Diffraction Study of the Plastic Deformation Mechanisms,” *Acta Mater*, **57**, 213 (2009).
- [26] R. Mahlangu, M.J. Phasha, H.R. Chauke, P.E. Ngoepe, “Structural, Elastic and Electronic Properties of Equiatomic PtTi as Potential High-Temperature Shape Memory Alloy,” *Intermetallics*, **33**, 1 (2013).
- [27] S. Pugh, “Relations Between the Elastic Moduli and the Plastic Properties of Polycrystalline Pure Metals,” *Philos. Mag*, **45**, 823 (1954).
- [28] K. Gschneidner, et al., “A family of Ductile Intermetallic Compounds,” *Nat. Mater.*, **2**, 587 (2003).
- [29] B. X. Z. Y. Tian, “Microscopic theory of hardness and design of novel superhard crystals,” *Int. J. Refr. Met. Hard Mater.*, **33**, 93 (2012).